Process of Destruction of Large Unilamellar Vesicles by a Zwitterionic Detergent, CHAPS: Partition Behavior between Membrane and Water Phases

Amornrat VIRIYAROJ, Hiroshi KASHIWAGI, and Masaharu UENO*

Faculty of Pharmaceutical Sciences, Toyama Medical and Pharmaceutical University; 2630 Sugitani, Toyama 930–0194, Japan. Received April 12, 2005; accepted June 9, 2005

The process of vesicle destruction by zwitterionic detergent, 3-[(3-cholamidopropyl)dimethylammonio]-1-propanesulfonate (CHAPS), was examined to clarify the vesicle-micelle transition mechanism. The physicochemical properties including turbidity, apparent particle size, Cl^- permeability, electron spin resonance (ESR) spectroscopic parameters, and freeze-fracture electron microscopy were investigated. The concentration of CHAPS was analyzed using HPLC to determine the partition coefficient during the solubilization process. The data obtained revealed that maximum turbidity and apparent particle size were found at the effective ratio (R_e) of 0.21 and 0.49, respectively. With a further increase in CHAPS concentration, turbidity and particle size abruptly decreased, suggesting the formation of mixed micelles. The partition coefficient changed throughout the solubilization process. In the presence of low concentrations of CHAPS, CHAPS partitioned into vesicles without destruction of membrane bilayers. When the $R_e<0.04$, the partition coefficient was independent of the detergent concentration with value of 24 M^{-1}. At R_e greater than 0.05, the membrane barrier abruptly decreased. At $0.04 \leq R_e < 0.21$, the gradual increase in the partition coefficient accounted for the occurrence of larger vesicles. In range of $0.21 \leq R_e < 0.52$, the abrupt increase in the partition behavior was possibly attributed to the structural change of mixed vesicles to mixed micelles. Furthermore, the ESR results showed that the incorporation of CHAPS into vesicles led to an increase in membrane fluidity near the polar head, and a decrease near the end of the acyl chain. ESR spectra of 5-doxylstearic acid in CHAPS-containing micelles were anisotropic, indicating that the steroidal structure of CHAPS was responsible for the micelles possessing an orderly arrangement of hydrocarbon chains.

Key words egg yolk phosphatidylcholine; vesicle–micelle transition; partition coefficient; 3-[(3-cholamidopropyl)dimethylammonio]-1-propanesulfonate (CHAPS); electron spin resonance

3-[(3-Cholamidopropyl)dimethylammonio]-1-propanesulfonate (CHAPS) is a zwitterionic detergent that was specifically designed for membrane biochemistry.[1] It is known to be a mild, nondenaturing detergent and is a derivative of natural bile salts. Its properties are of interest in several biochemical applications. These include the perturbation of membrane structures, membrane protein solubilization and functional reconstitution, and preparation of lipid vesicles with controlled size.[2—6]

The mechanism of vesicle destruction has been widely studied in connection with the reconstitution of membrane proteins after purification in detergent solutions.[7] It has been pointed out that several parameters are important for optimal reconstitution efficiency, *i.e.*, the type of detergent, detergent/phospholipid ratio, detergent/protein ratio, and salt concentration.[8] Therefore it is important to clarify the effects of detergent incorporated in the membrane phase on membrane properties. In the past decades much attention has been paid to the interaction of detergents with phospholipid membranes.[9—11] Octylglucoside, Triton X100, and bile acid derivatives were most widely studied.[12—14] Although CHAPS has been widely used in membrane biology, little is known of the details of the interaction of CHAPS and vesicles.

In a previous study in our laboratory on the solubilization of small unilamellar vesicles (SUV) by CHAPS, it was shown that small vesicles containing large amounts of CHAPS can fuse to increase their sizes during the solubilization process. Furthermore, when CHAPS was removed from mixed CHAPS/egg yolk phosphatidylcholine (EggPC) micelles, large vesicles formed by slow step-by-step dilution, but small vesicles formed by fast one-step dilution. The results demonstrated that the formation of large vesicles with the detergent removal method was related to the size growth of vesicles containing large amounts of detergent.[15]

In the present study, we report the solubilization process of large unilamellar vesicles (LUV) by CHAPS. The physicochemical properties including turbidity, apparent particle size, and Cl^- permeability were invesitigated. The partition behavior of CHAPS between the membrane phase and water phase was clarified. Additionally, electron spin resonance (ESR) spectroscopy of nitroxide derivatives of stearic acid at the 5- and 16-positions of the alkyl chain were used to determine the motional profiles at two main regions of the bilayers, near the polar head group and near the end of the hydrophobic chain, respectively.

Experimental

Materials EggPC (purity 98.8%) was purchased from NOF Corporation (Tokyo, Japan). 5- and 16-Doxylsteric acid (5-, 16-DS) were purchased from Aldrich Chemicals. Co. (U.S.A.). CHAPS was supplied by Dojindo Laboratories (Kumamoto, Japan). Sephadex G-75 was obtained from Pharmacia Biotech (Sweden). Dialysis membrane molecular weight cutoff 14000 was from Wako Pure Chemicals Industries (Tokyo, Japan). *N*-Tris(hydroxymethyl)methyl-2-aminoethanesulfonic acid (TES) and sodium chloride of analytical grade were purchased from Nacalai Tesque (Kyoto, Japan). All materials were used as received.

Preparation of LUVs EggPC was dissolved in chloroform–methanol (2 : 1, v/v), and the solvent was evaporated under a stream of nitrogen gas. The resulting lipid film was stored under a vacuum for at least 6 h to remove the residual solvent. Then the lipid film was hydrated with TES buffer (TES 20 mM and NaCl 150 mM, pH 7.0), yielding 25 mM of multilamellar vesicles (MLVs). The MLVs were frozen and thawed five times, then extruded through two stacked of 0.6-μm and 0.2-μm defined-pore polycarbonate fil-

* To whom correspondence should be addressed. e-mail: mueno@ms.toyama-mpu.ac.jp

ters (Nucleopore, Costar Co., U.S.A.) each 10 times, respectively, producing LUVs. After vesicle preparation, the actual phospholipid concentration was measured as phosphorous based on the method of Ames.[16] Thereafter, LUVs were diluted to 10 mM with TES buffer and used as stock LUV suspensions.

The LUVs were incubated with known concentration of CHAPS in TES buffer solution in a shaking water bath at 25 °C for 1 d using a dialysis cell composed of two compartments separated by a dialysis membrane.[17]

Size and Turbidity Measurement A quasi-elastic light scattering apparatus (LPA-3000/3100 laser particle analyzer, Otsuka Electronics, Osaka, Japan) was used to determine particle size and size distribution at 25 °C. The turbidity of mixed CHAPS/EggPC vesicles was measured as absorbance at 500 nm with a UV spectrometer (UV-160, Shimadzu, Japan). Samples were used without any dilution.

Chloride Permeation Cl^- permeability was determined by electrometric measurement of Cl^- efflux into $NaNO_3$ solution using an ion-selective electrode meter (Model 920 A, Orion Research, U.S.A.) with a Cl^--selective solid membrane electrode (Model 94-17 B). The column from Bio-Rad with dimensions of 1 cm×15 cm containing polyethylene support film was filled with Sephadex G-75 gel. The vesicles were separated from untrapped Cl^- by gel permeation chromatography equilibrated with an isotonic buffer, $NaNO_3$ 150 mM/TES buffer 20 mM (pH 7.0). If Cl^- obeys first-order kinetics[17,18]:

$$\ln(C_\infty - C_t) = \ln(C_\infty - C_0) - kt \quad (1)$$

where k is the rate constant for permeation of Cl^-, C_t is the measured Cl^- concentration at time t, C_0 is the initial Cl^- concentration, and C_∞ is the Cl^- concentration after complete liberation of entrapped Cl^- obtained by adding 20% Tritron X100. k is calculated as the slope of the line obtained by plotting $\ln(C_\infty - C_t)$ against t.

The permeability coefficient (p) for Cl^- was obtained from relation:

$$p/k = (\text{internal volume/vesicle})/(\text{membrane area/vesicle}) \quad (2)$$

CHAPS Analysis and Apparent Partition Coefficient For quantification of CHAPS, a sample from the vesicle-free compartment of the dialysis cell was adjusted to an appropriate concentration by the addition of purified water, and then 50 μl of sample was injected onto the HPLC column (Waters LC Module I^{plus}, U.S.A.). A C-18 reverse-phase column (Inertsil ODS 5 μm, column dimension 25 cm×4.6 mm, GL Sciences, Japan) was used as the stationary phase. A mixture containing acetronitrile 400 ml and water 600 ml was used as the mobile phase. The flow rate was 0.7 ml/min. The UV detector was set at 210 nm. The total amount of CHAPS before adding to the dialysis cell was also analyzed using HPLC. The concentration of CHAPS aggregated in the membrane phase was determined. The effective ratio (R_e) can be calculated according to the equation

$$R_e = D_B/L \quad (3)$$

where D_B is the concentration of CHAPS in the membrane phase and L is the concentration of EggPC.

The partition coefficient (K) was defined by Eq. 4.

$$K = X/D_W = D_B/(L+D_B)D_W \quad (4)$$

where X is the mole fraction of detergent in the membrane phase and D_W is the concentration of detergent in the water phase in equilibrium.

ESR Spectroscopy 5-DS or 16-DS was dissolved in methanol. An appropriate spin probe was placed into the bottom of a test tube to make a molar ratio of N-DS/EggPC=1 : 100. The methanol was evaporated under a steam of nitrogen gas to give a thin film of spin probe on the wall of the test tube. Thereafter the film was stored under a vacuum for at least 6 h for removal of residual methanol.[19,20] The 200 μl of sample was added into the test tube containing a thin film of the spin label. The sample was gently swirled and left for more than 2 h before measurement to ensure that the spin probe was distributed throughout the mixed aggregates. ESR spectra (X band, 100 kHz modulation) were recorded on a JES TE 100 ESR spectrometer (JEOL, Japan) at 25 °C. The conditions were set as follows: microwave power, 12 mW; modulation amplitude, 0.1 mT; amplitude, 79 and 63, for 5-DS and 16-DS, respectively; sweep width, ±5 mT; sweep time 4 min; time constant, 0.1 s. The order parameter (S) of 5-DS was calculated using the Gaffney equation.[21]

$$S = \frac{T_\parallel' - (T_\perp' + C)}{T_\parallel' + 2(T_\perp' + C)} \times 1.723 \quad (5)$$

$$C = 1.4 - 0.053(T_\parallel' - T') \text{ gauss}$$

where $T_\parallel'$ and T' are outer hyperfine splitting and inner hyperfine splitting, respectively.

The rotational correlation time (τ_c) of 16-DS was calculated from the following equation.[22]

$$\tau_c\,(\text{s}) = 6.5\times10^{-10} H_0 [(I_0/I_{-1})^{1/2} - 1] \quad (6)$$

where H_0 is the width in gauss of central field spectrum line, I_0 is the peak-to-peak height of the central field line and I_{-1} is the peak-to-peak amplitude of the high field line.

Freeze-Fracture Electron Microscopy Specimens for freeze-fracture microscopy were prepared according to the procedure previously reported.[23] Samples were rapidly frozen in liquid nitrogen and then was fractured at −120 °C with a freeze replica apparatus (FR-7000B, Hitachi, Tokyo Japan). After fracturing the samples, an electric discharge was applied to deposit Pt/C and then C on the surface of the fractured sample at angles of 45° and 90°, respectively. The replicas were removed from the holder by submersion in a solution of commercial bleach and distilled water. The cleaned replicas were mounted on 300-mesh Ni grids, dried, and investigated with a transmission electron microscope (JEM200 CX, JEOL, Tokyo, Japan).

Results

Effect of CHAPS on Turbidity and Apparent Particle Size of EggPC Vesicles Figure 1 shows the changes in turbidity and apparent particle size against the R_e at 25 °C. These two curves represent different breakpoints. At low concentrations of CHAPS, the turbidity and apparent particle size remained close to those of CHAPS-free vesicles. With the addition of CHAPS concentration up to the R_e=0.14, the turbidity started to increase. The turbidity steeply increased and the maximum turbidity was found at the R_e of 0.21. A further increase in CHAPS concentration led to a precipitous decrease in turbidity, while the particle size increased from 173 nm (R_e=0) to about 237 nm (R_e=0.25—0.45) in the downward turbidity curve. A sharp increase in apparent particle size was observed at R_e=0.49. Above this R_e value, the turbidity and particle size drastically decreased, suggesting the formation of mixed micelles.

Membrane Barrier Efficiency Figure 2 represents the permeability coefficient of Cl^- ion through the vesicle membrane at different R_e values. The permeability of CHAPS-free vesicles was about 8.6×10^{-11} cm s^{-1}. When CHAPS was incorporated at $R_e \geq 0.05$, the Cl^- permeability was rather small. With an increase in CHAPS concentration, the Cl^- permeability markedly increased at $R_e \geq 0.086$. The percentage of Cl^- retention in the vesicles decreased more than 20% within 20 min at R_e=0.086 (data not shown). These indicate that the barrier efficiency of vesicle membrane was signifi-

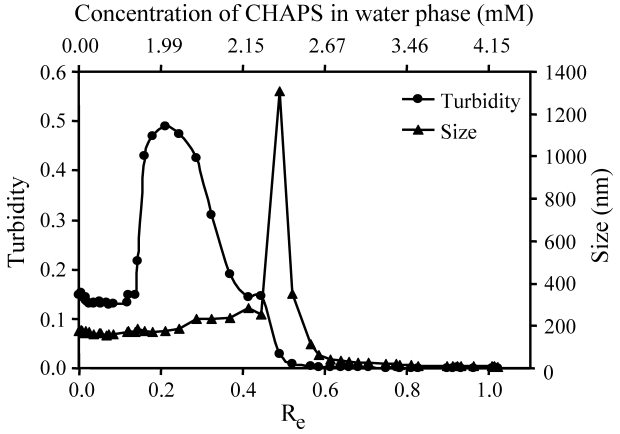

Fig. 1. Changes in Turbidity at 500 nm (●) and Apparent Particle Size (▲) of EggPC Vesicles as a Function of the Effective Ratio of CHAPS to EggPC (R_e) at 25 °C

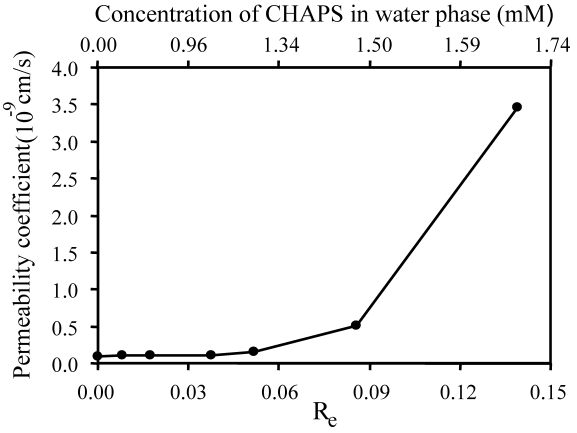

Fig. 2. Plot of Permeability Coefficient of Cl^- Ion through the Vesicle Membrane against Effective Ratio (R_e) at 25 °C

cantly reduced.

Partition Equilibrium of CHAPS between the Membrane Phase and Water Phase Since the physicochemical parameters used to characterize the interaction between lipid bilayers and detergents critically depend on the partition of detergents into the lipid phase, we performed a CHAPS partition experiment between the membrane phase and water phase. The CHAPS concentration was analyzed using HPLC. The retention time of CHAPS was 6.4—6.8 min. The concentration of CHAPS in the membrane phase was calculated. Figure 3 shows the partition behavior of CHAPS in the membrane phase and water phase. The ordinate of Figs. 3a and b represents the CHAPS concentration in the mole fraction in the membrane phase, and the abscissa shows that in the water phase obtained using the equilibrium dialysis method. The slope of this curve represents the apparent partition coefficient. In the low CHAPS concentration region, a linear relationship was obtained. The experimental result shows that the slope is 24 M^{-1}. During $0.04 \leq R_e < 0.21$ (point A—B), the apparent partition coefficient gradually increased while the turbidity started to increase and reached maximum turbidity, as depicted in Fig. 3a. At $0.21 \leq R_e < 0.52$ (point B—C), the apparent partition coefficient abruptly increased while the turbidity drastically decreased. In this range, the macroscopic phase separation occurred within 8-h standing after equilibrium dialysis, as represented in Fig. 4. The complete phase separation was performed by centrifugation at 2000 ***g*** for 15 min. The lower phase was clearly viscous liquid representing the formation of intermediate aggregates or mixed micelles.

Behavior of Nitroxide Spin Probes during Vesicle Destruction The ESR spectra of 5-DS and 16-DS in TES buffer are isotropic, as shown in Figs. 5a and 6a, respectively. Since the nitroxide molecule can rotate rapidly in buffer solution, sharp triplet bands are obtained. Figures 5b and 6b represent the ESR spectra of 5-DS and 16-DS in CHAPS-free EggPC vesicles, respectively. The ESR spectrum of 5-DS in EggPC vesicles represents the anisotropic spectrum, suggesting that the mobility of the spin probe is restricted in vesicles. These ensure that the spin probe is immobilized inside the membrane bilayers. The fluidity of the membrane can be estimated from the outer hyperfine spitting. As can be seen from Figs. 5b—e, all ESR spectra of 5-DS are anisotropic at

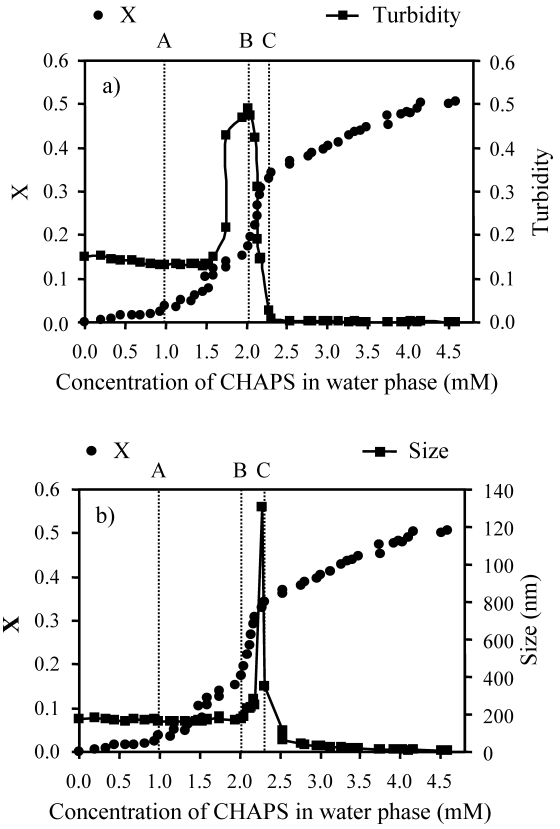

Fig. 3. Partition of CHAPS between the Membrane Phase and Water Phase at 25 °C

a) Dependence of X (●) and turbidity at 500 nm (■) on CHAPS concentration in the water phase. b) Dependence of X (●) and apparent particle size (■) on CHAPS concentration in the water phase. The R_e values at points A, B, and C are 0.04, 0.21 and 0.52, respectively.

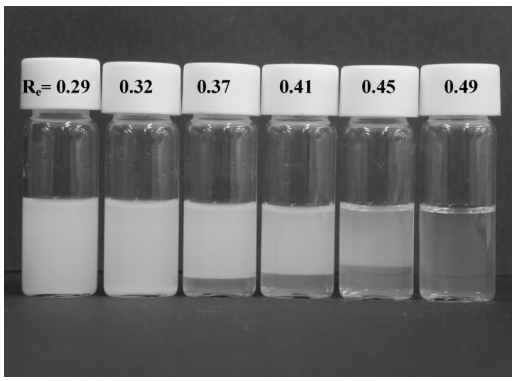

Fig. 4. Photographs of CHAPS/EggPC Mixed Aggregates at R_e=0.29, 0.32, 0.37, 0.41, 0.45, and 0.49, Respectively

The spontaneous macroscopic phase separation occurred within 8-h standing after 24 h equilibrium dialysis.

$R_e < 1.02$, although the addition of CHAPS in the membrane resulted in the shortening of the outer hyperfine spitting. The order parameters of CHAPS-containing EggPC vesicles are shown in Fig. 7. At a low R_e of CHAPS in the membrane, the order parameters were more or less constant. The order parameter started to decrease at $R_e \geq 0.25$, indicating the beginning of the destruction of lamellar structures. On the other hand, the ESR spectrum of 16-DS in EggPC vesicles represents the isotropic spectrum at $0 \leqq R_e \leqq 1.02$. With increasing

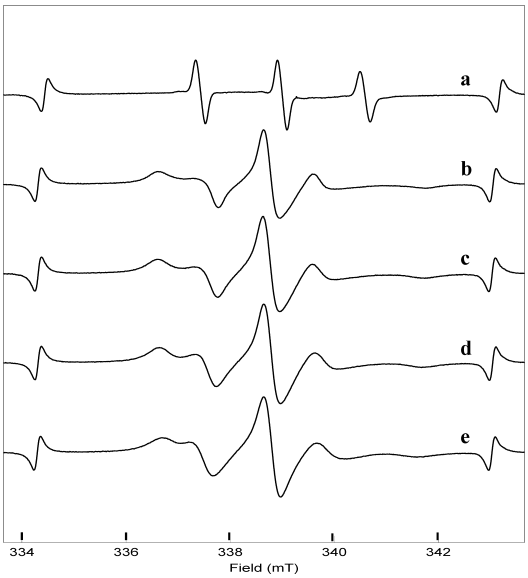

Fig. 5. ESR Spectra of 5-DS in a) TES Buffer; b) EggPC Vesicles; and CHAPS/EggPC Mixed Aggregates at R_e=c) 0.21, d) 0.49, and e) 1.02, Respectively, at 25 °C

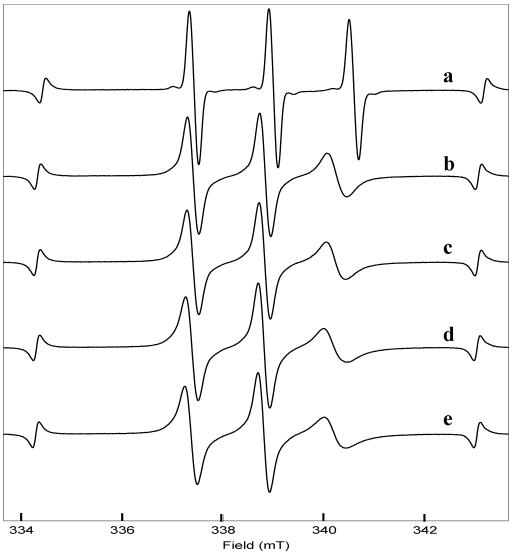

Fig. 6. ESR Spectra of 16-DS in a) TES Buffer; b) EggPC Vesicles; and CHAPS/EggPC Mixed Aggregates at R_e=c) 0.21; d) 0.49; and e) 1.02, Respectively at 25 °C

CHAPS concentration, the height of the high field line decreased, leading to an increase in the rotational correlation time (Fig. 6e). The sharp increase in the rotational correlation time was found in range of R_e=0.25—0.52, as depicted in Fig. 8. The increase in rotational correlation time means a decrease in fluidity at the end of the acyl chain of PC during the solubilization process.

Freeze-Fracture Electron Microscopy Figure 9 illustrates freeze-fracture electron micrographs of CHAPS-free vesicles and of CHAPS-containing EggPC vesicles. Figure 9a depicts a freeze-fracture micrograph of CHAPS-free vesicles. Spherical LUVs are mainly observed. A comparison between Figs. 9a and b shows that no significant morphologic changes in vesicles occurred after the addition of a small amount of CHAPS. At R_e=0.16, large vesicles with rough

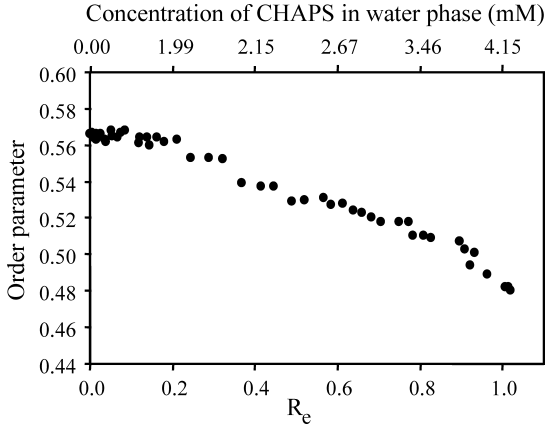

Fig. 7. Dependence of Order Parameter of 5-DS in the Equilibrated CHAPS-Containing EggPC Vesicles on the Effective Ratio (R_e) during the Solubilization Process at 25 °C

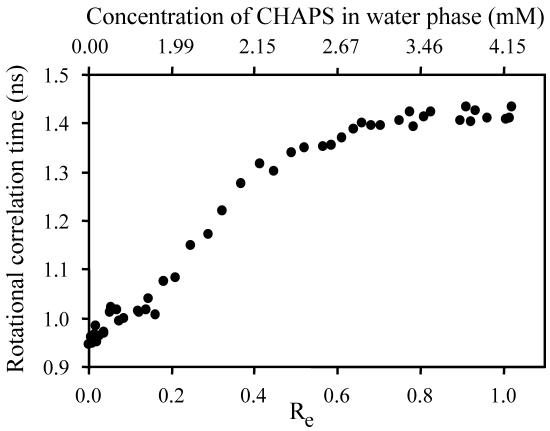

Fig. 8. Dependence of Rotational Correlation Time of 16-DS in the Equilibrated CHAPS-Containing EggPC Vesicles on the R_e during the Solubilization Process at 25 °C

surfaces and the formation of small vesicles were found (Fig. 9c). The appearance of small vesicles has previously been observed upon the addition of octylglucoside into EggPC vesicles by our group.[24] We tentatively named these small vesicles containing high amounts of detergent SUVs* to distinguish them from SUVs formed using the sonication method. With increasing CHAPS concentration up to R_e=0.21, the aggregation and fusion of SUVs* were observed, indicating that a rapid detergent-induced fusion of vesicles occurred (Fig. 9d). With a further increase in CHAPS concentration up to R_e=0.29, the coexistence of vesicles and rodlike micelles was observed (Fig. 9e). It should be noted that the number of vesicles significantly decreased with the increase in the R_e of CHAPS and that the disappearance of vesicles was observed at R_e=0.49, as shown in Fig. 9f. Furthermore, the replica at R_e=0.61 showed small particles (Fig. 9g). At this point the turbidity and apparent particle size were small. It is therefore conceivable that the small particles were mixed micelles.

Discussion

The dialysis technique was adopted to avoid possible solubilization by direct addition of a detergent and to obtain the monomer concentration of the detergent in equilibrium between vesicles and buffer solution. The cmc (critical micelle

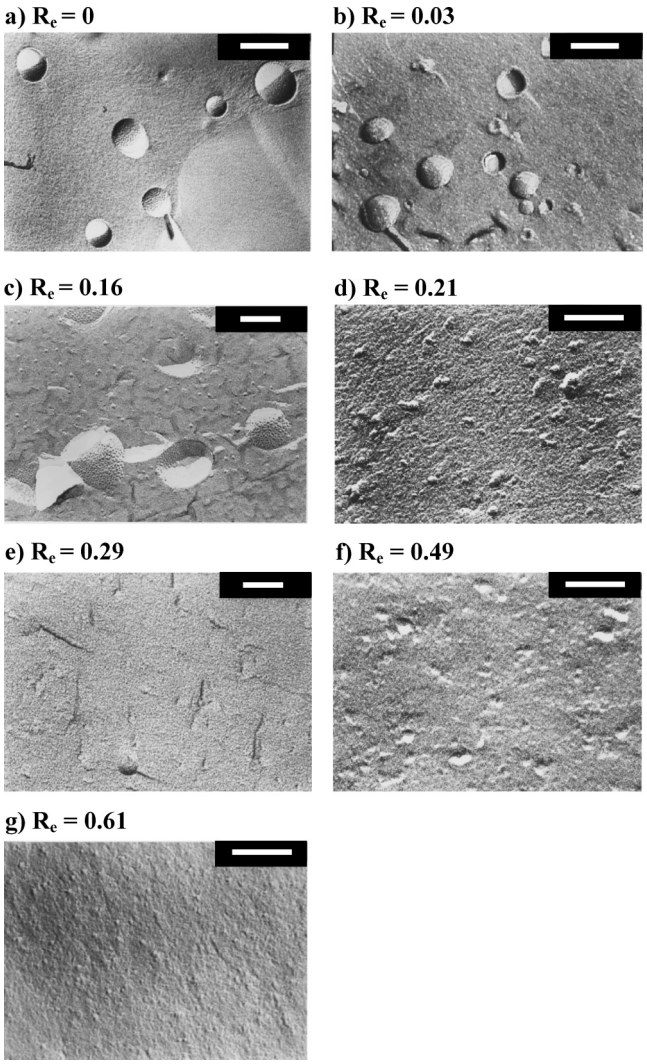

Fig. 9. Freeze-Fracture Electron Micrographs of CHAPS-Containing EggPC Vesicles at R_e=a) 0; b) 0.03; c) 0.16; d) 0.21; e) 0.29; f) 0.49; and g) 0.61, Respectively. Bar represents 200 nm.

concentration) values of CHAPS were 6.21 and 5.94 mM in presence of NaCl 100 and 200 mM, respectively.[25] In this experiment, the concentrations of CHAPS in the water phase were less than 4.6 mM in all cases, thereby confirming that the physicochemical changes during solubilization were due to the insertion of CHAPS monomer into bilayers. In the presence of low concentrations of CHAPS, CHAPS partitions to vesicles without destruction of the membrane. In accordance with the data on turbidity and apparent particle size, the freeze-fracture electron replica confirmed that the morphologic integrity of bilayers was still preserved at R_e=0.03 (Fig. 9b). Further addition of CHAPS resulted in a steep increase in the Cl^- permeability coefficient (Fig. 2). In this area, the destruction of vesicles has not yet occurred. The reduction of membrane barrier efficiency attributed to the incorporation of detergents into EggPC vesicles resulting in leakage of entrapped materials has previously been reported.[26—28] Our freeze-fracture electron microscopy observations revealed SUVs* appeared. Thus another possible explanation of the increment in membrane permeability before vesicle destruction in the CHAPS–EggPC vesicle system was due to the breakdown of LUVs into SUVs*. When the CHAPS concentration increased up to R_e=0.21, the fusion of SUVs* was observed (Fig. 9d). The appearance of fusion of SUVs* upon the addition of CHAPS into EggPC lipsomes is in agreement with the system of octylglucoside–EggPC liposomes in our previous studies.[24,29] However, the fusion of small vesicles containing large amounts of sodium cholate was not observed.[15,30] The discrepancy in the fusion of vesicles during solubilization can be explained by the net charge of detergent molecule. Since CHAPS is a zwitterionic detergent that has no net charge in its molecule. Therefore small vesicles containing large amounts of CHAPS are easily fusible.

Turbidity is an indicator of the number of particles, average diameter, and structural change in mixed vesicles.[31] Upon the addition of CHAPS to EggPC vesicles, the turbidity increased considerably and reached the maximum value. A further increase in the CHAPS concentration led to a precipitous decrease in turbidity. From the freeze-fracture electron micrographs, no mixed micelles were observed during an upward of turbidity curve (Figs. 9c, d). This result agrees with those of a previous study by Almog *et al.* showing that the liposome suspension was essentially vesicular within the upward turbidity curve in octylglucoside–EggPC system.[9] In the region of the downward turbidity curve, the EggPC content in the nonvesicular portion increased after centrifugation, defining the destruction of vesicles (data not shown).

The change in apparent particle size represented a pattern similar to the turbidity curve (Fig. 1). Apparently, these two curves showed different characteristic changes. In the region of the downward turbidity curve, the apparent particle size obviously increased from 173 nm (R_e=0) to 237 nm (R_e=0.25—0.45). Additionally, the mixed aggregates in this area provided a broad size distribution leading to a decrease in the homogeneity of the system. The formation of rod-like micelles is responsible for the decrease in turbidity coinciding with an increase in apparent particle size. These mixed micelles were 140—370 nm in length (Fig. 9e). When the apparent particle size was approximately 1300 nm at R_e=0.49, the turbidity decreased to nearly zero, suggesting destruction of the vesicles. The direct information from freeze-fracture electron microscopy revealed that most of the lamellar structures had disappeared. Very high viscosity is thought to account for the obviously large size analyzed with a quasi-elastic light-scattering apparatus.

The plot of the mole fraction of CHAPS in the membrane phase (X) *versus* CHAPS concentration in the water phase (D_w) describes the change in partition coefficient during the solubilization process (Figs. 3a, b). This observation is consistent with our previous work and that of other groups performed in an octylglucoside/PC system.[12,17,33] At a low concentration of CHAPS, a rather small value of the apparent partition coefficient of CHAPS into vesicles was obtained. At $0.04 \leq R_e < 0.21$ (point A—B), the partition coefficient gradually increased. The large vesicles at R_e=0.16 (Fig. 9c) can explain an increase in the partition coefficient in this range. At $0.21 \leq R_e < 0.52$ (point B—C), the partition coefficient strongly increased as a function of R_e. This implies that an increase in CHAPS in the membrane phase in this domain accounted for a transformation of the lamellar structure to rod-like micelles. The coexistence of vesicles and mixed micelles in freeze-fracture electron microscopy images supports

the partition coefficient data (Fig. 9e). With a further increase in CHAPS concentration of $R_e \geq 0.52$ (point C), the samples were optically transparent solutions, suggesting complete solubilization. From the data obtained, it can be stated that the detergent-saturated bilayers (R_e sat) and detergent-solubilized bilayer (R_e sol) of CHAPS are 0.21 and 0.52, respectively. Under similar experimental conditions, the R_e sat and R_e sol values of octylglucoside observed in our previous study were 1.2 and 3.0, respectively.[33] The comparison in terms of R_e sat and R_e sol of CHAPS to those of octylglucoside indicated that the solubilization efficiency of CHAPS is higher than that of octylglucoside.

ESR is a useful technique to determine fluidity and structural changes in lipid bilayers. Generally, the incorporation of detergent into the bilayers increases the molecular disorder and mobility of the hydrocarbon chains.[34] Different spin-labeling positions in stearic acid were used to investigate membrane properties. 5-DS was used to determine the behavior of membranes near the polar head group, while 16-DS was used for that at the end of hydrophobic chain during the solubilization process. As illustrated in Figs. 5b—e, ESR spectra of 5-DS are anisotropic throughout the whole process of the EggPC vesicle solubilization by CHAPS, including the stage of mixed micelles (stage 4). ESR spectra of 5-DS in sodium cholate- and sodium taurocholate-containing EggPC micelles were also found to be anisotropic (data not shown). On the other hand, ESR spectra of 5-DS in EggPC/octylglucoside and EggPC/octaethyleneglycol mono-*n*-dodecyl ether systems gradually changed from slightly fluid anisotropic bands to highly fluid isotropic ones as the vesicle solubilization proceeded. In addition, a considerably larger order parameter of 5-DS in EggPC micelles containing a minimal amount of CHAPS (0.53, Fig. 7) than that of 5-DS in EggPC micelles containing a minimal amount of octylglucoside (0.50)[29,35] indicates considerably less membrane fluidity of CHAPS-containing micelles than usual mixed micelles (*e.g.* EggPC/octylglucoside micelles). Moreover, the order parameter of 5-DS in CHAPS-containing EggPC micelles decreases markedly with a further increase in R_e in the micelle stage, reaching 0.48 at $R_e = 1.02$ (Fig. 7). Throughout these vesicle solubilization processes, the presence of the steroidal structure in CHAPS might result in orderly arrangement of hydrophobic hydrocarbon chains in EggPC micelles and in decreased membrane fluidity. Since the ESR spectra of 16-DS are isotropic (Fig. 6) and those of 5-DS are anisotropic (Fig. 5), the membrane fluidity at the end of hydrocarbon chains is greater than that near the polar head group throughout the whole process of vesicle solubilization. In our other experiment using octylglucoside as a detergent, it was found that the decrease in both the order parameter and rotational correlation time led to an increase in membrane fluidity near the polar head and end of the acyl chain in the system of octylglucoside-EggPC vesicles (data not shown). The contradictory result in membrane fluidity at different positions in the CHAPS/EggPC system could be explained by the the steroidal skeleton structure of CHAPS affecting the degree of orientation at the end of the acyl chain. This result is consistent with the results of our previous study showing that the rotational correlation time of 12-DS increased after the addition of sodium cholate to EggPC liposomes.[36]

In summary, we propose the destruction mechanism of LUVs by CHAPS as follows: stage 1 is the distribution of CHAPS through vesicle membranes. No significant structural change is observed. Stage 2 is the formation of uneven LUVs with the appearance of SUVs* and the fusion of SUVs*; stage 3 is the coexistence of vesicles and rod-like micelles; and stage 4 is the transformation of vesicles to spherical mixed micelles. In this report, we found that the fusion of SUVs* is responsible for the growth of vesicles during solubilization. This could thus explain why the vesicles prepared by dialysis of CHAPS–EggPC mixed micelles yielded large vesicles. The size growth is a crucial factor not only to clarify the mechanism of vesicle-micelle transition but also to control the preparation in the functional reconstitution of membrane proteins.

References

1) Hjelmeland L. M., U.S. Patent 4372888 (1983).
2) Aeed P. A., Sperry A. E., Young C. L., Nagiec M. M., Elhammer A. P., *Biochemistry*, **43**, 8483—8493 (2004).
3) Cladera J., Rigaud J., Villaverde J., Dunach M., *Eur. J. Biochem.*, **243**, 798—809 (1997).
4) Boadu E., Sager G., *Biochim. Biophys. Acta*, **1509**, 467—474 (2000).
5) Rotenberg M., *J. Colloid Interface Sci.*, **144**, 591—594 (1991).
6) Lasic D. D., Martin F. J., Neugebauer J. M., Kratohvil J. P., *J. Colloid Interface Sci.*, **133**, 539—544 (1989).
7) Paternostre M., Roux M., Riguad J., *Biochemistry*, **27**, 2668—2677 (1988).
8) Nakanishi M., Tetsuka T., Kagawa Y., Moriyama A., Sasaki M., Hirata H., *Biochim. Biophys. Acta*, **115**, 193—200 (1993).
9) Almog S., Litman B. J., Wimley W., Cohen J., Wachtel E. J., Barenholz Y., Ben-Shaul A., Lichtenberg D., *Biochemistry*, **29**, 4582—4592 (1990).
10) Edwards K., Gustafsson J., Almgren M., Karlsson G., *J. Colloid Interface Sci.*, **161**, 299—309 (1993).
11) Walter A., Vinson P., Kaplun A., Talmon Y., *Biophys. J.*, **60**, 1315—1325 (1991).
12) Paternostre M., Meyer O., Grabiella-Madelmont C., Lesieur S., Ghanam M., *Biophys J.*, **69**, 2476—2488 (1995).
13) Spink C. H., Lieto V., Mareand E., Pruden C., *Biochemistry*, **30**, 5104—5112 (1991).
14) López O., Maza A., Coderch L., López-Iglesias Wehrli E., Parra J. L., *FEBS Lett.*, **426**, 314—318 (1998).
15) Sun C., Ueno M., *Colloid Polym. Sci.*, **278**, 855—863 (2000).
16) Ames B. N., *Methods Enzymol.*, **8**, 115—117 (1966).
17) Ueno M., *Biochemistry*, **28**, 5631—5634 (1989).
18) Sun C., Hanasaka A., Kashiwaki H., Ueno M., *Biochim. Biophys. Acta*, **1467**, 18—26 (2000).
19) Almeida L. E., Borissevitch I. E., Yushmanov V. E., Tabak M., *J. Colloid Interface Sci.*, **203**, 456—463 (1998).
20) Yuann J. P., Morse R., *Biochim. Biophys. Acta*, **1416**, 135—144 (1999).
21) Sefton B. M., Gaffney B. J., *J. Mol. Biol.*, **90**, 343—358 (1974).
22) Cruz A., Marsh D., Pérez-Gil J., *Biochim. Biophys. Acta*, **1415**, 125—134 (1998).
23) Sriwongsitanont S., Ueno M., *Colloid Polym Sci.*, **282**, 753—760 (2004).
24) Ueno M., Akechi Y., *Chem. Lett.*, **1991**, 1801—1804 (1991).
25) Chattopadhyay A., Harikumar K. G., *FEBS Lett.*, **391**, 199—202 (1996).
26) Lasch J., Hoffmann J., Omelyanenko W. G., Klibanov A. A., Torchilin V. P., Binder H., Gawrisch K., *Biochim. Biophys. Acta*, **1022**, 171—180 (1990).
27) Ueno M., Tanford C., Reynolds J. A., *Biochemistry*, **23**, 3070—3076 (1984).
28) Ueno M., *Biochim. Biophys. Acta*, **904**, 140—144 (1987).
29) Ueno M., Hirota N., Kashiwagi H., Sagasaki S., *Colloid Polym. Sci.*, **282**, 69—75 (2003).
30) Ueno M., Kashiwagi H., Hirota N., *Chem. Lett.*, **1997**, 217—218 (1997).
31) Lambert O., Levy D., Ranck J., Leblanc G., Rigaud J., *Biophys. J.*, **74**, 918—930 (1998).

32) Opatowski E., Kozlov M. M., Lichtenberg D., *Biophys. J.*, **73**, 1448—1457 (1997).
33) Ueno M., *Membrane*, **18**, 96—106 (1993).
34) Goñi F. M., Alonso A., *Biochim. Biophys. Acta*, **1508**, 51—68 (2000).
35) Kashiwagi H., Sagasaki S., Tanaka M., Aizawa K., Sun C., Ueno M., "Studies in Surface Science and Catalysis," Vol. 132, ed. by Iwasawa Y., Oyama N., Kunieda H., Elsevier, Amsterdam, 2001, pp. 603—606.
36) Sun C., Kasiwagi H., Ueno M., *Chem. Pharm. Bull.*, **50**, 1145—1150 (2002).